CHEFFLER
MMERMANN

23rd International Conference on

THE PHYSICS OF

VOL. 2

23rd International Conference on

THE PHYSICS OF SEMICONDUCTORS

Volume 2

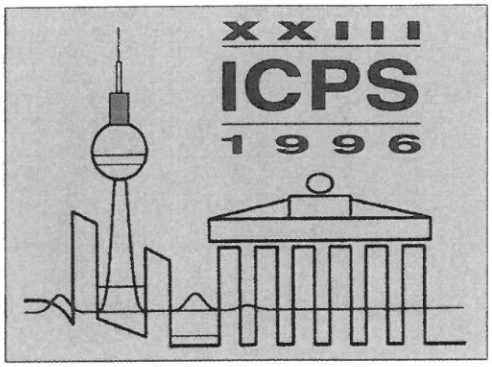

Berlin, Germany
July 21 – 26, 1996

Editors
MATTHIAS SCHEFFLER
ROLAND ZIMMERMANN

World Scientific

298

PSEUDOPOTENTIAL THEORY OF SEMICONDUCTOR QUANTUM DOTS, WIRES, AND FILMS

Alex Zunger
National Renewable Energy Laboratory, Golden, Colorado 80401, USA
E-mail: alex_zunger@nrel.gov

ABSTRACT

The electronic structure of nanostructures is almost universally addressed by the "standard model" of effective-mass k·p envelope function approach. While eminently successful for quantum wells, this model breaks down for small structures, in particular, for small dots and wires. Until recently, it was impractical to test the "standard model" against more general approaches that allow for many-band (Γ-X-L) coupling. However, it is now possible, due to special tricks, to apply the all-band plane-wave pseudopotential method to 10^3 - 10^4 atom nanostructures. This shows (I) how the "standard model" fails, in some cases, (ii) how size effect lead to a reduction in dielectric constants and to band gaps that differ from what is expected in effective-mass theory, (iii) the emergence of a "zero-confinement state" in 2D films, (iv) that small dots of III-V materials have an indirect gap that converts to direct above the critical size, (v) how the spectra of CdSe dots evolve from the bulk, and (vi) how the electron-hole Coulomb energy is overestimated by the effective-mass wavefunctions.

1 Introduction

Optoelectronic applications[1] often exploit electronic properties of artificial heterostructures, such as superlattices and quantum wells, with characteristic dimensions of 100 Å. Their electronic properties could, in principle, be interpreted using the same tool applied successfully to bulk solids, namely, a complete band structure. Nanostructure single-particle energies and wave functions would then be solutions to

$$\{\frac{\hat{p}^2}{2m} + V(r)\}\psi(r) = \epsilon\psi(r) \quad . \tag{1}$$

where $V(\mathbf{r})$ is the total three-dimensional *atomistic* potential, including all effects of the interfaces between materials *A* and *B* for the *A/B* heterostructures. $V(\mathbf{r})$ could be computed self-consistently from the occupied states using, e.g., density functional theory, or it could be approximated as a superposition of screened atomic potentials, i.e.,

$$V(\boldsymbol{r}) = \sum_{i,\boldsymbol{R}} V_i(\boldsymbol{r},\boldsymbol{R},\boldsymbol{d}_i) \tag{2}$$

for atom species i at basis site $\mathbf{d}_i$ in cell $\mathbf{R}$. Because of the very large number of monolayers spanning ~100 Å nanostructures, they have until very recently[2] been beyond the reach of such *direct* electronic structure calculations [Eqs. (1)-(2)], the conventional computational effort for which scales as the *cube* of the number of atoms. The spectroscopy of nanostructures was instead interpreted using an approach so common that we term it the "standard model": either the simple effective-mass approximation (EMA), or the k·p method together with the envelope-function approximation (EFA). The k·p approach uses a perturbation theory description of band dispersion for pure *A* or *B* within a small set of near-edge bands identified as physically relevant. Although it has been eminently successful in a variety of applications[1], often overlooked formal restrictions on the standard model, compromise its description of an *A/B* heterostructure. The fact that its parameters are usually fit to experimental data has also made it difficult to appraise these limitations. In this paper I first describe some interesting differences between the electronic properties of nanostructures as described by direct pseudopotential diagonalization [Eqs. (1)-(2)] vs. the more approximate "standard model". I then use the pseudopotential model to discuss some properties of dots, wires, and films.

2 Method of Calculation

In the direct pseudopotential approach[2], Eqs. (1)-(2) are solved explicitly. The screened atomic pseudopotentials $\{v_i\}$ are fit to *measured* bulk band structure, deformation potentials, and effective masses, to the *measured* surface work functions, and to the *calculated* local-density-approximation (LDA) wavefunctions of the bulk. This new-generation "semiempirical pseudopotentials"[3] thus have LDA-quality wavefunctions (and matrix elements), yet the energies are realistic, so no "LDA error" occurs. We use the potentials of Refs. 2, 4, 5, and 6 for Si[2], GaAs/AlAs[4], CdSe[5], and InP[6], respectively. The wavefunctions $\{\psi_i\}$ are expanded in a plane-wave basis in a supercell geometry, using the same cut-off energy as used in fitting the pseudopotentials to the bulk properties. The surface dangling-bonds are passivated by a saturating pseudopotential. The eigenvalue problem (1) is solved via the "folded spectrum method"[2] that allows one to find eigensolutions in a given "energy window" (e.g., near-edge), rather than being forced by the orthogonality principle to find *all* eigensolutions. This trick thus enables us to calculate for 1,000-10,000 atom nanostructures the near-edge energies and wavefunctions *exactly*, with a computational cost comparable to that of ≈10 atom unit cells, using conventional methods.

For comparison, we have also solved the 8-band k·p equations for superlattices. We use the implementation of Baraff and Gershoni et al.[7], except that the input Luttinger parameters are recalculated from our semiempirical pseudopotentials. This assures that the comparison of the electronic structure of superlattices between k·p and the direct pseudopotential diagonalization reflects the differences in the methods, not in the inputs.

3 k·p vs. Direct Diagonalization Results for (001)$(AlAs)_n/(GaAs)_n$ Superlattices

Unlike the "standard model", our 'plane-wave basis direct diagonalization approach' includes all-band couplings and, at the same time, envelope function or effective-mass approximations are avoided. Such direct single-particle calculations of the electronic properties of small quantum structures (superlattices, films, and dots) have produced[8,9] novel features that escaped the standard 8-band k·p approach. For (001)$(GaAs)_n/(AlAs)_n$ superlattices, such unexpected features include:

(I) The even-odd oscillations of the energies of L-folded state $\bar{R}(L)$ and $\bar{X}(L)$ with the period n,

(ii) The red shift ("deconfinement") of the $\bar{\Gamma}(\Gamma)$ conduction band at short periods,

(iii) The interaction, repulsion, and crossing of the two lowest conduction bands $\bar{\Gamma}(\Gamma)$ and $\bar{\Gamma}_{(X_z)}$ (Γ-folded and X_z-folded, respectively) at a critical superlattice period n_c,

(iv) The significant *quantitative* overestimate of the position of the $\bar{\Gamma}(\Gamma)$ conduction band with respect to direct diagonalization,

(v) Significant *quantitative* underestimate of the position of the hh2 and split-off bands with binding energies ≥200 meV[8], including incorrect out-of-plane dispersion and position of avoided crossing,

(vi) Omission of the spin-splitting for the in-plane dispersion of the valence bands[8], and

(vii) Overestimation of the mass-anisotropy $m_{\parallel}/m_{\perp}$ at Γ for both electrons and holes[8,9].

While it was generally expected that the "standard model" will fail for small nanostructures (e.g., short-period superlattices), direct diagonalization studies[8,9] have shown that the situation is not so simple. For example, the *hh*1 and *lh*1 valence band energies of $(GaAs)_n/(AlAs)_n$(001) superlattices are accurately described by the "standard model" even down to the $n = 1$ monolayer superlattice limit, while the conduction bands at Γ and X are poorly described even at $n \approx 20$. This is so because the standard k·p model describes poorly the strong coupling of *bulk* X_{1c} and Γ_{1c} at the superlattice *conduction* band minimum. On the other hand, the coupling between the

bulk X_{1v} and Γ_{15v} at the superlattice *valence* band maximum (also described poorly) happens to be weak, so its misrepresentation is inconsequential. Incorrect description of inter-valley coupling of folded states is also the reason for the significant errors made by the k·p model in describing the values of the effective-mass tensor, the deformation potential[10] and the wavefunction[11] of InP/GaP superlattices.

4 Direct-indirect Crossover for GaAs Dots, Wires, and Films

In this section we contrast the electronic properties of (a) AlAs-embedded and (b) free-standing GaAs quantum films, wires, and dots using our direct pseudopotential method[12,13]. We find that, quite surprisingly (Fig. 1), the confinement energy of the valence-band maximum (VBM) is larger in AlAs-embedded than in free-standing (hydrogen passivated) quantum structures, due to the "zero-confinement" character[14] of the VBM in the latter case. We also find[12,13] that the VBM is always localized on GaAs (insert to Fig. 2). As for the CBM, *small* GaAs quantum structures always have an *indirect* band gap. In the case of free-standing quantum structures, the conduction-band minimum (CBM) of small structures originates from the GaAs X_{1c} conduction state, thus making the quantum structure

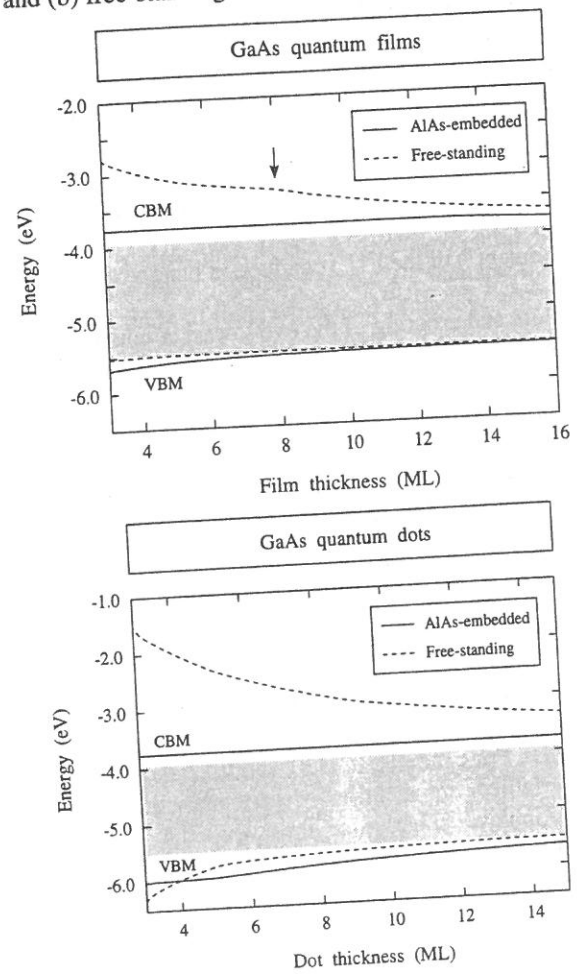

FIG. 1. Band-edge energies of AlAs-embedded (solid lines) and free-standing (dashed lines) GaAs quantum films, (top) and quantum dot (bottom) as a function of thickness. The shaded area denotes the GaAs bulk band gap. From Ref. 13.

maximum (also described poorly)
consequential. Incorrect description
reason for the significant errors
the effective-mass tensor, the
InP/GaP superlattices.

ires, and Films

properties of (a) AlAs-embedded
and dots using our direct pseudopo-

FIG. 1. Band-edge energies of AlAs-embedded (solid lines) and free-standing (dashed lines) GaAs quantum films, (top) and quantum dot (bottom) as a function of thickness. The shaded area denotes the GaAs bulk band gap. From Ref. 13.

tential method[12,13]. We find that, quite surprisingly (Fig. 1), the confinement energy of the valence-band maximum (VBM) is larger in AlAs-embedded than in free-standing (hydrogen passivated) quantum structures, due to the "zero-confinement" character[14] of the VBM in the latter case. We also find[12,13] that the VBM is always localized on GaAs (insert to Fig. 2). As for the CBM, *small* GaAs quantum structures always have an *indirect* band gap. In the case of free-standing quantum structures, the conduction-band minimum (CBM) of small structures originates from the GaAs X_{1c} conduction state, thus making the quantum structure

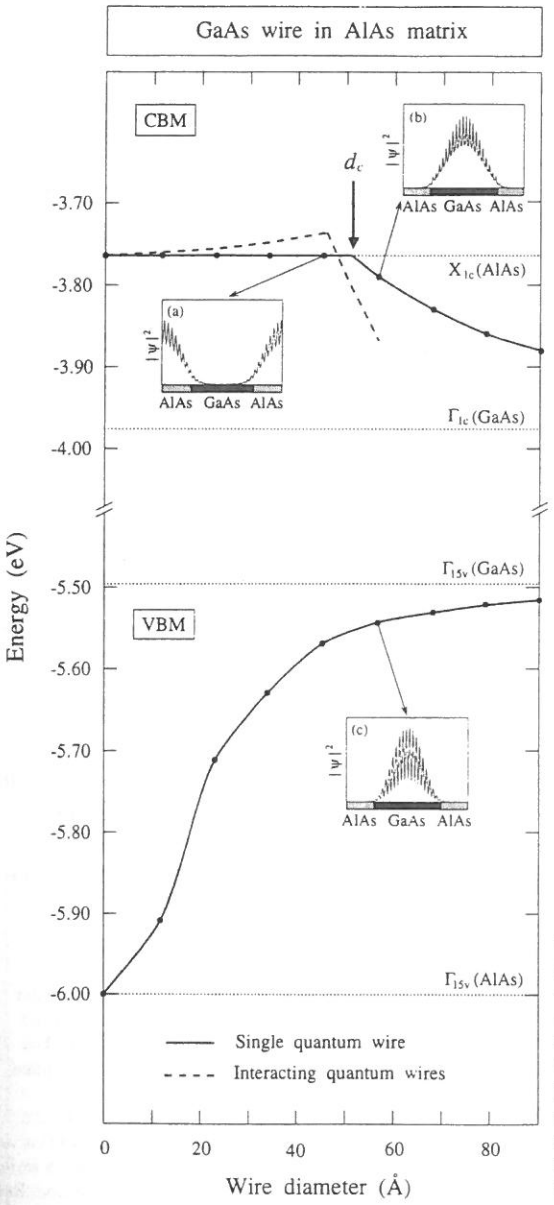

intrinsically indirect (type-I alignment in real space). In the case of small, AlAs-embedded quantum structures, the CBM originates from the X_{1c} conduction state that is localized in the AlAs matrix, leading to a type-II alignment in real space (insert to Fig. 2). *Large* GaAs quantum structures, on the other hand, have a *direct* band gap, with the CBM originating from the GaAs Γ_{1c} state (type-I in real and reciprocal space). Thus, for both free-standing and AlAs-embedded GaAs quantum structures we predict an indirect → direct transition as the size increases; the critical size for this transition (Table I) is larger in AlAs-embedded than in free-standing quantum structures.

FIG. 2. The VBM and CBM energies of an isolated GaAs cylindrical quantum wire embedded in an AlAs matrix, calculated with the pseudopotential method, are shown as a function of the wire diameter (solid dots connected by line). The CBM energy of a periodic square array of GaAs wires in AlAs is also shown (dashed line); the period of the array is $D = 57$ Å. Insets show the wave-function amplitude of the VBM and the CBM. From Ref. 12.

Table I. Critical sizes (in ML) for the indirect → indirect crossover in free-standing and AlAs-embedded GaAs quantum films, wires, and dots. From Ref. 16.

	Film	Wire	Dot
Free-standing	8	14	>15
AlAs-embedded	13	25	>15

5 Band Gaps of CdSe

Figure 3 compares our calculated excitonic band gap of CdSe dots[5] with experiment[15]. The results without an electron-hole Coulomb term (solid dots) differ considerably from the results with this term (crosses). The dielectric constant (Fig. 3a) is significantly different form the bulk value. Note (Fig. 3b) how the EMA over-estimates considerably the observed band gap.

We attribute this good agreement to the use of a realistic *microscopic* hamiltonian [Eqs. (1)-(2)].

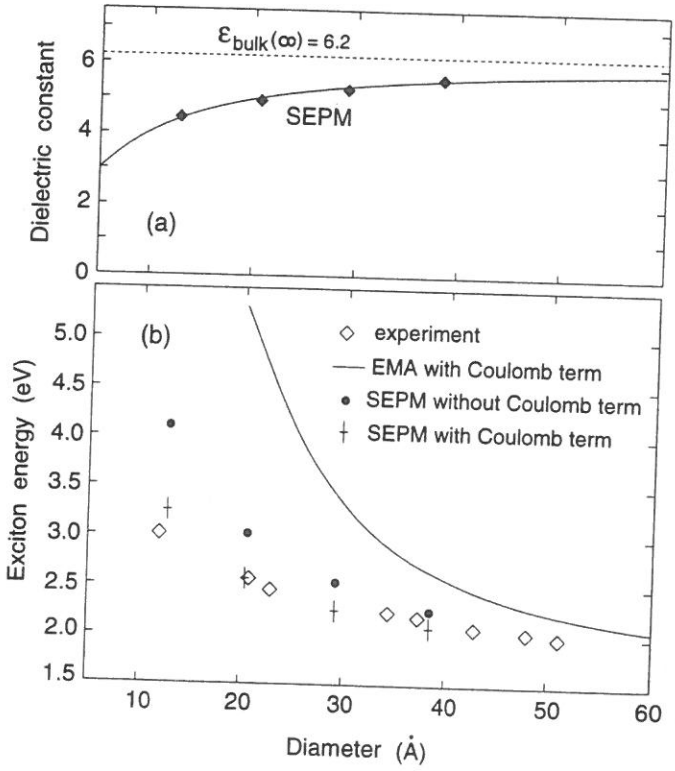

FIG. 3. CdSe quantum dot dielectric constant (a) and exciton energies (b). The solid line in (a) is the fitted result of Eq.(1). The experimental data and the effective mass (EMA) curve in (b) are from Ref. 15 while the calculations are from Ref. 5.

→ indirect crossover in free-standing
, wires, and dots. From Ref. 16.

Wire	Dot
14	>15
25	>15

)nic band gap of CdSe dots[5] with
le Coulomb term (solid dots) differ considerably from the results with this term (crosses). The dielectric constant (Fig. 3a) is significantly different form the bulk value. Note (Fig. 3b) how the EMA over-estimates considerably the observed band gap.

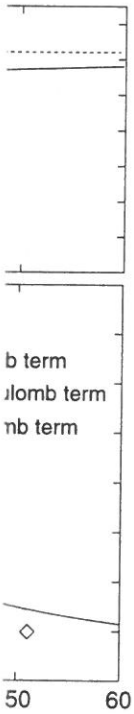

We attribute this good agreement to the use of a realistic *microscopic* hamiltonian [Eqs. (1)-(2)].

FIG. 3. CdSe quantum dot dielectric constant (a) and exciton energies (b). The solid line in (a) is the fitted result of Eq.(1). The experimental data and the effective mass (EMA) curve in (b) are from Ref. 15 while the calculations are from Ref. 5.

6 The Exciton Coulomb Energy of Si, GaAs, and CdSe Quantum Dots

The excitonic energy for nanostructures contains a single-particle band-gap part $Eg\alpha R^{-2}$ (in the absence of electron-hole interaction), as well as electron-hole contributions, including Coulomb $E_{coul}\sim R^{-1}$. In the single particle approximation

$$E_{coul} = \frac{e^2}{\varepsilon}\int \frac{|\psi_h(r_h)|^2|\psi_e(r_e)|^2}{|r_h - r_e|} d^3r_e d^3r_h \qquad (3)$$

where ψ_h and ψ_e are hole and electron single-particle wavefunction. In bulk and in partially confined systems $E_{coul} = 0$, but in dots, it can be large. Given the significant difference between EMA and the microscopic (pseudopotential) wavefunctions, we have decided to calculate E_{coul} from both. The results[16] are shown in Table II. It shows that the EMA overestimates the Coulomb energy by as much as 50%, and that εE_{coul} has a *sublinear* dependence on 1/R.

Table II. Calculated Product of Dielectric Constant ϵ by the Coulomb Energy using Pseudopotential and EMA Wavefunctions

System size (Å)	$\varepsilon E_{coul}^{ps}$	$\varepsilon E_{coul}^{EMA}$
Spherical Si Dots:		
14.2	2.67	3.65
17.2	2.00	3.00
20.3	1.74	2.53
Rectangular GaAs Dots:		
8.0	2.84	4.84
12.0	2.12	3.23
16.0	1.70	2.42
20.0	1.42	1.93
24.0	1.19	1.61
28.0	1.05	1.38
32.0	0.94	1.21
44.0	0.70	1.08
Cubic CdSe Dots:		
7.7	3.50	5.73
15.3	2.08	2.87
23.0	1.49	1.91

A direct pseudopotential approach can be used to predict quantitatively many electronic properties of semiconductor nanostructures in agreement with experiment, but sometimes in conflict with simpler effective-mass and k·p results.

Acknowledgments

I would like to thank H. Fu, A. Franceschetti, L.W. Wang, and D. M. Wood on fruitful and enjoyable collaborations on this subject.

References

1. See, e.g., *Nanostructures and Quantum Effects*, Springer Series in Materials Science **31** (Springer-Verlag, Berlin, 1994).
2. L.-W. Wang and A. Zunger, J. Phys. Chem. **98**, 2158 (1994); Phys, Rev. Lett. **73**, 1039 (1994); J. Chem. Phys. **100**, 2394 (1994).
3. L.-W. Wang and A. Zunger, *Phys. Rev. B* **51**, 17,398 (1995).
4. K. A. Mäder and A. Zunger, *Phys. Rev. B* **50**, 17,393 (1994).
5. L.-W. Wang and A. Zunger, *Phys. Rev. B* **53**, 9579 (1996).
6. H. Fu and A. Zunger, *Phys. Rev. B* (submitted).
7. G. A. Baraff and D. Gershoni, *Phys. Rev. B* **43**, 4011 (1991).
8. D. M. Wood and A. Zunger, *Phys. Rev. B* **53**, 7950 (1996).
9. D. M. Wood, A. Zunger, and D. Gershoni, *Europhys. Lett.* **33**, 383 (1996).
10. A. Franceschetti, S.-H. Wei, and A. Zunger, *Phys. Rev. B* **52**, 13,992 (1995).
11. A. Franceschetti, S.-H. Wei, and A. Zunger, *Phys. Rev. B* **50**, 8094 (1994).
12. A. Franceschetti and A. Zunger, *Phys. Rev. B* **52**, 14,664 (1995).
13. A. Franceschetti and A. Zunger, *Appl. Phys. Lett* **68**, 3455 (1996).
14. S. B. Zhang and A. Zunger, *Appl. Phys. Lett.* **63**, 1399 (1993); *Phys. Rev. B* **48**, 11,204 (1993); *Superlatt. & Microstruct.* **14**, 141 (1994).
15. C. B. Murray, D. J. Norris, and M. G. Bawendi, *J. Am. Chem. Soc.* **115**, 8706 (1993).
16. A. Franceschetti and A. Zunger (unpublished).